Int J Clin Exp Pathol 2015;8(4):3491-3502
www.ijcep.com /ISSN:1936-2625/IJCEP0006530

Original Article

CB2R orchestrates fibrogenesis through regulation of inflammatory response during the repair of skeletal muscle contusion

Miao Zhang[1], Shu-Kun Jiang[1], Zhi-Ling Tian[1], Meng Wang[1], Rui Zhao[1,2], Lin-Lin Wang[1], Shan-Shan Li[1], Min Liu[1], Jiao-Yong Li[1], Meng-Zhou Zhang[1], Da-Wei Guan[1,2]

[1]Department of Forensic Pathology, China Medical University School of Forensic Medicine, Shenyang 110122, Liaoning Province, P. R. China; [2]Remote Forensic Consultation Center, Collaborative Innovation Center of Judicial Civilization, China University of Political Science and Law, Beijing 100192, P. R. China

Received January 31, 2015; Accepted March 24, 2015; Epub April 1, 2015; Published April 15, 2015

Abstract: Skeletal muscle injuries repair typically is an overlapping event between inflammation and tissue repair. Our previous study has demonstrated that activation of cannabinoid receptor type 2 (CB2R) by JWH-133 alleviates fibrosis in the repair of rat skeletal muscle contusion. Meanwhile, accumulated data show that CB2R stimulation exerts anti-inflammatory property in sepsis and cystitis. However, the effects of CB2R on inflammatory cytokines in response to the repair of skeletal muscle contusion are still unknown. In this study, we used selective agonist or antagonist of CB2R to observe the role of CB2R on inflammation and fibrogenesis during the repair of contused skeletal muscles in rats. Our results revealed that treatment with Gp1a, a selective CB2R agonist, significantly decreased the infiltration of neutrophils and macrophages, the expression of pro-inflammatory cytokines MCP-1, TNF-α, IL-1β and IL-6, the expression of pro-fibrotic cytokines IL-4, IL-13, TGF-β and P-Smad3 while increased anti-fibrotic cytokine IL-10 production as compared with Vehicle. The opposite results were observed in the CB2R inhibition group with AM630. Our study demonstrated that CB2R orchestrates fibrogenesis through regulation of inflammatory response during the repair of skeletal muscle contusion.

Keywords: CB2R, inflammation, fibrosis, skeletal muscle injury, wound repair

Introduction

Repair of skeletal muscle injuries is a multifactor regulated healing process and can be divided into acute phase, repair phase and remodeling phase [1]. Within each phase, a myriad of orchestrated reactions and interactions between cells and chemicals are put into action. The whole process includes necrosis of the damaged muscle fibers, recruitment of inflammatory cells, activation of myogenic cells to differentiate and fuse into new myofibers as well as appearance of myofibroblasts to form fibrotic lesion [2]. It was reported that the extent of the early inflammatory response after skeletal injuries may be excessive and causes edema with resultant anoxia and further cell death [3]. Furthermore, excessive inflammation and repair can trigger an excessive accumulation of extracellular matrix (ECM) components, providing inappropriate signals for cell differentiation, which leads to the formation of a permanent fibrotic scar [4].

The endogenous cannabinoid system is composed of cannabinoid receptor types 1 and 2 (CB1R and CB2R), their endogenous ligands (endocannabinoids) and enzymes that synthesize and degrade endocannabinoids. CB1R is expressed in high abundance in central nervous system [5], while CB2R is predominantly expressed in peripheral tissues and cells including liver, lymphocytes and neutrophils [6, 7]. Furthermore, our previous study has found that CB2R is also expressed in skeletal muscles, macrophages and myofibroblasts during the repair of skeletal muscle contusion [8, 9]. CB2R stimulation dampens LPS-induced pro-inflammatory cytokine production in the model of acute experimental sepsis in mice [10], reduces

the inflammatory cells infiltration and attenuates fibrosis in cirrhotic rats [6], and prevents the development of skin and lung fibrosis in a mouse model of systemic sclerosis [11]. Conversely, CB2R knockouts developed enhanced inflammation and tissue injury [12], and inhibition of CB2R signaling augments bleomycin-induced dermal fibrosis in mice [13]. These evidences demonstrate that CB2R is closely involved in inflammatory response and tissue repair.

Fibrosis is closely related to inflammatory response in wound healing [14]. Our previously study has demonstrated that treatment with selective CB2R agonist JWH-133 decreased fibrogenesis in rat contusion model [9], we speculated that the anti-fibrotic effect of CB2R stimulation on the repair of skeletal muscle contusion may be due to its anti-inflammatory effect. In this study, we used a highly selective CB2R agonist Gp1a and CB2R antagonist AM630 to verify the hypothesis.

Materials and methods

Animal model of skeletal muscle contusion

All animal protocols were conformed to the 'Principles of Laboratory Animal Care' (National Institutes of Health publication no. 85-23, revised 1985) which seeks to minimize both the number of animals used in a procedure and any suffering that they might experience, and were performed according to the Guidelines for the Care and Use of Laboratory Animals of China Medical University. A reproducible muscle contusion model in rats was established previously in our laboratory [8]. Briefly, 90 healthy adult Sprague-Dawley male rats, weighing between 280 and 300 g were anesthetized by intraperitoneal injection with 2% sodium pentobarbital (30 mg/kg). The right hindlimb was fixed on a board in a prone position by extending the knee and dorsiflexing the ankle to 90°. A single impact at velocity of 3 m/s was delivered to the gastrocnemius and soleus muscles of the right posterior limb. The size of impact interface of the counterpoise (weighing 500 g) was 1.127 cm^2. Each rat was individually housed in a cage and fed regular laboratory chow with water supplied *ad libitum*. A 12-hour day and night cycle was maintained. Rats were sacrificed by intraperitoneal injection of an overdose of sodium pentobarbital (350 mg/kg) at 1, 3, 5, 7, 9, and 14 days after contusion (5 rats in each time point). Each muscle specimen was taken from wound site and equally divided into two blocks. One block was used for morphological evaluation, and another was used for molecular biological detection. No bone fracture was detected at dissection. Besides, 1 healthy adult Sprague-Dawley male rat without contusion was used as control for normalization in Western-blotting.

Treatments with CB2R agonist and antagonist

90 rats were randomly divided into 3 groups (30 rats/group) according to treatments with Gp1a (highly selective CB2 agonist, Ki: 0.037 nM and 353 nM for CB2 and CB1 receptors, respectively; Tocris Bioscience, Ellisville, MO, USA), AM630 (CB2 antagonist/inverse agonist, Ki = 31.2 nM, displays 165-fold selectivity over CB1 receptors; Tocris Bioscience, Ellisville, MO, USA), or the Vehicle alone. Gp1a and AM630 were dissolved in a Vehicle containing saline: DMSO: Tween-80 in an 18:1:1 ratio. Gp1a, AM630 and Vehicle were injected at 30 minutes after contusion and once a day for 13 days post-injury by intraperitoneal injection (Gp1a, 10 mg/kg; AM630, 5 mg/kg). Rats injected with equal volume of Vehicle (2 ml/kg) were used as controls. At 1, 3, 5, 7, 9 and 14 days after contusion, 5 animals of each group were sacrificed. The doses and treatments were based on previous studies and preliminary experiment (Figure S1) [15-17].

Immunohistochemical staining and morphometric analysis

Fixed muscle specimens were embedded in paraffin. 5 μm-thick sections were prepared from paraffin-embedded tissue. Immunostaining was performed using the streptavidin-peroxidase method. The sections were deparaffinized in xylene, hydrated with a series of graded alcohol, and then heated in 0.01 mol/L sodium citrate buffer (pH 6.0) in a medical microwave oven for antigen retrieval. Subsequently, 3% hydrogen peroxide was applied for suppressing endogenous peroxidase activity. The sections were blocked with 10% non-immune goat serum to reduce non-specific binding. Then tissue sections were incubated with primary antibody, including rabbit anti-myeloperoxidase (MPO) polyclonal antibody (dilution 1:500; Ab65871, Abcam, Cambridge, UK), mouse anti-CD68 monoclonal antibody (dilution 1:100; ab31630, Abcam, Cambridge,

UK), and mouse anti-alpha-smooth muscle actin (α-SMA) monoclonal antibody (dilution 1:200; Ab7817, Abcam, Cambridge, UK) overnight at 4°C, followed by incubation with Histostain-Plus kit according to the manufacturer's instructions (Zymed Laboratories, South San Francisco, CA, USA). The sections were routinely counterstained with hematoxylin. As immunohistochemical controls for immunostaining procedures, some sections were incubated with normal rabbit or mouse IgG, or phosphate buffered saline (PBS) in place of the primary antibodies. In addition, hematoxylin-eosin (H&E) staining and Masson's trichrome staining were conventionally conducted.

Sections containing the largest contusion area were analyzed. MPO, CD68 and α-SMA positive cells were calculated under the 400-fold magnification in the contusion zones. Five fields in the contusion zones were randomly chosen for the calculations or evaluations in each section. All measurements and data analysis were performed independently by two pathologists in a blind manner. Morphometrical analysis was performed using Image-Pro Plus 6.0 (Media Cybernetics, Rockville, USA).

Protein extraction and immunoblotting assay

The skeletal muscle samples were ground into powder with liquid nitrogen using a grinder and homogenized with a sonicator in RIPA buffer (KGP9100, KeyGEN BioTECH, Nanjing, China) containing protease inhibitors and phosphatase inhibitors at 4°C. Homogenates were centrifuged at 12,000× g for 10 min three times at 4°C, and the resulting supernatants were collected. Protein concentrations were determined using the bicinchoninic acid method. Aliquots of the supernatants were diluted in an equal volume of 6x electrophoresis sample buffer and boiled for 5min. Protein lysates (30 μg) were separated on a 12% sodium dodecyl sulfate-poly-acrylamide electrophoresis gel and transferred onto polyvinylidene fluoride membranes (Millipore, Billerica, MA, USA). After being blocked with 5% BSA in Tris-buffered saline with Tween-20 at room temperature for 2 h, the blots were incubated with rabbit anti-transforming growth factor-β (TGF-β) polyclonal antibody (dilution 1:400; 3711S, CST, Cambridge, UK), rabbit anti-phospho-small mother against decapentaplegic-3 (P-Smad3) (dilution 1:10000; PAB11304, Abnova, Taipei, Taiwan) or rabbit anti-GAPDH polyclonal antibody (dilution 1:2500; ab9485, Abcam, Cambridge, UK) at 4°C overnight and horseradish peroxidase conjugated goat anti-rabbit IgG (sc-2004, Santa Cruz Biotechnology, CA, USA) at 1:2,000 dilution at room temperature for 2 h. The blotting was visualized with Western blotting luminol reagent (sc-2048, Santa Cruz Biotechnology, CA, USA) and by the Electrophoresis Gel Imaging Analysis System (MF-ChemiBIS 3.2, DNR Bio-Imaging Systems, ISR). Subsequently, densitometric analyses of the bands were semi-quantitatively conducted using Scion Image software (Scion Corporation, MD, USA).

Cytokines and chemokines analysis

A Quantibody Rat Inflammation Array 1 (QAR-INF-1-4, RayBiotech, Inc, Norcross, GA, USA) and skeletal muscle protein lysate were used to simultaneously determine the expression of 10 cytokines: interleukin (IL) -1α, IL-1β, IL-2, IL-4, IL-6, IL-10, IL-13, monocyte chemoattractant protein 1 (MCP-1), interferon-γ (IFN-γ), and tumor necrosis factor-α (TNF-α). Each cytokine was arrayed in quadruplicate, together with positive and negative controls. Cytokine standards at predetermined concentrations were used to generate a 5-point standard curve. Before addition of standard or sample cytokines, the glass chip was blocked by incubation with 100 μL sample diluent for 30 mins. The cytokine standards or samples (100 μL) were added and incubated at room temperature for 1 h. After a washing step, 80 μL of detection antibody was added (1 h at room temperature) followed by a further washing step before the addition of 80 μL of Cy3-conjugated streptavidin for 1 h. Fluorescent signals were visualized with a laser scanner (Axon GenePix; Molecular Devices, Sunnyvale, CA) set at 532-nm excitation. Data were extracted with RayBio Q Analyzer software (RayBiotech, Inc). The background intensity was subtracted prior to analysis. After subtracting background signals and normalization to positive controls, comparison of signal intensities for antigen-specific antibody spots between groups were utilized to determine relative differences in expression levels of each sample.

Total RNA extraction and quantitative real-time PCR

Total RNA was isolated from the skeletal muscle specimens with RNAiso Plus (9108, Takara Biotechnology, Shiga, Japan) according to the

Table 1. Quantitative real-time PCR primer sequences

Gene	Primer		GenBank ID
Gapdh	Forward	5'-CATCTCCCTCACAATTCCATCC-3'	NM_017008.4
	Reverse	5'-GAGGGTGCAGCGAACTTTAT-3'	
Col1a1	Forward	5'-GCTTGAAGACCTATGTGGGTATAA-3'	NM_053304.1
	Reverse	5'-GGGTGGAGAAAGGAACAGAAA-3'	
Col3a1	Forward	5'-CAGGCCAATGGCAATGTAAAG-3'	NM_032085.1
	Reverse	5'-GCCATCCTCTAGAACTGTGTAAG-3'	

manufacturer's instructions. OD values of each RNA sample were measured by ultraviolet spectrophotometer. A260/A280 ranged from 1.8 to 2.0. Then, the RNA (250 ng) was reverse-transcribed into cDNA using the PrimeScript™ RT reagent Kit (RR037A, Takara Biotechnology, Shiga, Japan). The resulting cDNA was used for quantitative real-time PCR with the sequence-specific primer pairs for *Col1a1*, *Col3a1* and *Gapdh* (**Table 1**; Takara Biotechnology, Shiga, Japan). Quantitative real-time PCR amplification was performed by ABI 7500 Real-Time PCR System (Applied Biosystems, Foster City, CA) using SYBR® PrimeScript™ RT-PCR Kit (RR081A, Takara Biotechnology, Shiga, Japan) followed by the parameters: 2 μL cDNA was loaded to each quantitative real-time PCR reaction. A denaturing step was at 95°C for 30 s followed by 15 s at 95°C, 34 s at 60°C, 15 s at 95°C, 60 s at 60°C, 15 s at 95°C for 40 cycles. PCR-generated fragments for *Col1a1*, *Col3a1* and *Gapdh* primer sets were 89, 108 and 100 bp, respectively. Dissociation curve analysis of PCR products revealed single peaks, indicating specific amplification products. The relative expression levels of *Col1a1* and *Col3a1* were normalized by subtracting the corresponding *Gapdh* threshold cycle (C_T) values using the $\Delta\Delta C_T$ comparative method [18].

Statistical analysis

Results were expressed as mean ± standard deviation (SD), and statistical significance was determined by two-way analysis of variance using PRISM 6.0 software (GraphPad Software, Inc.). Data were considered significantly different for $P < 0.05$.

Results

Effects of CB2R on inflammatory cell infiltration

Hemorrhage, edema and necrosis were microscopically detected in the contusion zones at the early stages of inflammatory response in all three groups. A large number of inflammatory cells infiltrated into the contusion zones at 1 and 3 days post-injury in H&E-stained sections (**Figure 1**).

Neutrophils or macrophages were identified by immunostaining of MPO or CD68, respectively (**Figure 2A-F**). Compared to rats in the Vehicle group, significant decrease of neutrophils in number was observed in the Gp1a group at 1 day post-injury ($P < 0.05$; **Figure 2G**), and macrophages at 1, 3 and 5 days post-injury ($P < 0.01$; **Figure 2H**), while infiltrated neutrophils increased in the AM630 group at 1 day post-injury ($P < 0.05$; **Figure 2G**), and macrophages at 1 and 3 days post-injury ($P < 0.05$; **Figure 2H**).

Effects of CB2R on the expression of cytokines and chemokines

Rat Inflammation Array 1 and Western-blotting were employed to detect the expression of cytokines and chemokines in different groups. The tendency of decreases in the MCP-1 and TNF-α expression and increases in the IL-1β, IL-4 and IL-10 expression were found in all evaluated periods. It was noted that the expression of IL-6 peaked at 3 days, TGF-β and P-Smad3 at 5 days, and IFN-γ at 3 and 14 days post-injury, respectively (**Figures 3**, **4**).

Compared to the Vehicle group, Rat Inflammation Array 1 showed significantly falls in the MCP-1 and IL-6 expression in the Gp1a group at 1, 3 and 5 days post-injury ($P < 0.01$; **Figure 3A**, **3D**), as well as TNF-α at 1 and 3 days ($P < 0.01$; **Figure 3B**); IL-1β at 3 and 5 days ($P < 0.05$; **Figure 3C**); IL-13 at 5, 7 and 9 days ($P < 0.01$; **Figure 3G**) and IFN-γ expression at 3 days ($P < 0.01$; **Figure 3H**) post-injury, respectively, and increases in the IL-10 expression at 5, 9, 14 days ($P < 0.01$) and 7 days ($P < 0.05$; **Figure 3F**); IFN-γ expression at 9 and 14 days ($P < 0.01$; **Figure 3H**) post-injury. In the AM630 group, the assays showed increases in the MCP-1 expression at 1 and 3 days post-injury ($P < 0.01$; **Figure 3A**), as well as TNF-α at 1, 3 and 5 days ($P < 0.05$; **Figure 3B**); IL-1β at 7 and 9 days ($P < 0.05$; **Figure 3C**); IL-4 at 7 and 9 days ($P < 0.01$; **Figure 3E**); IL-6 at 1 and 3 days ($P < 0.05$; **Figure 3D**); IL-13 at 5 ($P < 0.01$) and 7 days ($P < 0.05$; **Figure 3G**) and IFN-γ expression

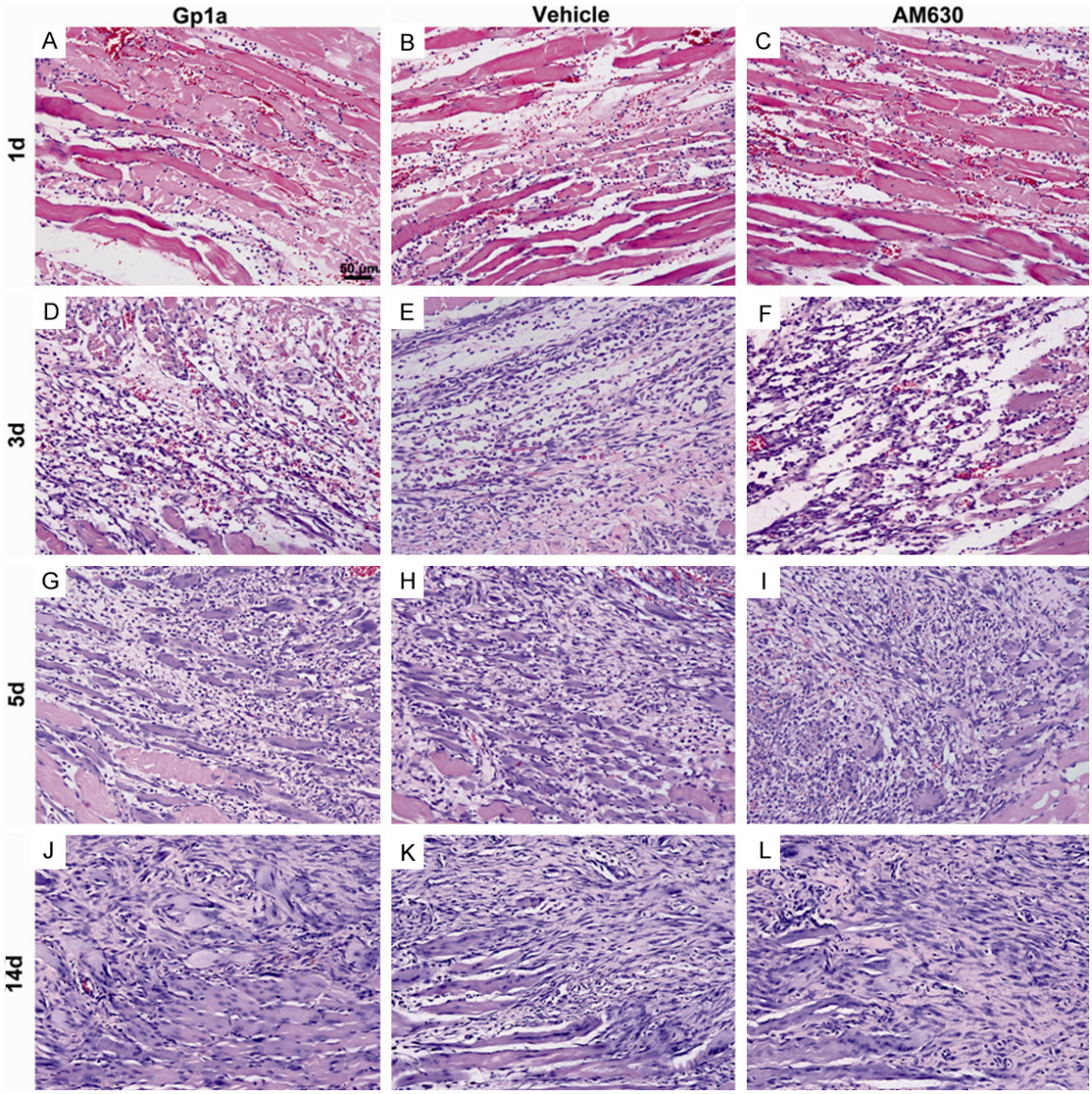

Figure 1. The dynamic histopathological changes of injured skeletal muscles by H&E staining. A-C represent findings at 1 day post-injury in Gp1a, Vehicle and AM630 group, respectively. Hemorrhage, edema, and necrosis are observed in contused skeletal muscles, and a few of round-shaped mononuclear cells (MNCs) and polymorphonuclear cells (PMNs) are seen in the contusion zone. D-F represent changes at 3 days after injury. Spindle-shaped fibroblasts (FBCs) are present in the injured tissue, and damaged muscle fibers are mostly eliminated. G-I represent findings at 5 days post-injury. Centronucleated regenerating myofibers are present in the injured tissue in all the three groups. J-L represent changes at 14 days post-injury. A large number of FBCs, concomitantly with centronucleated regenerating myofibers, accumulate in the contusion zone (original magnification, ×200).

at 3 days ($P < 0.01$; **Figure 3H**). There was no significant difference in IL-1α or IL-2 level in all evaluated periods among the three groups (data not shown).

Western-blotting showed significantly decreases of TGF-β expression in the Gp1a group at 3 days ($P < 0.05$) and 7 days ($P < 0.01$) post-injury (**Figure 4B**), as well as P-Smad3 expression at 3, 5 days ($P < 0.01$) and 7 days ($P < 0.05$) post-injury (**Figure 4C**). Conversely, significantly increases in the TGF-β expression was observed in the AM630 group at 3, 5 days ($P < 0.01$) and 7 days ($P < 0.05$; **Figure 4B**), as well as P-Smad3

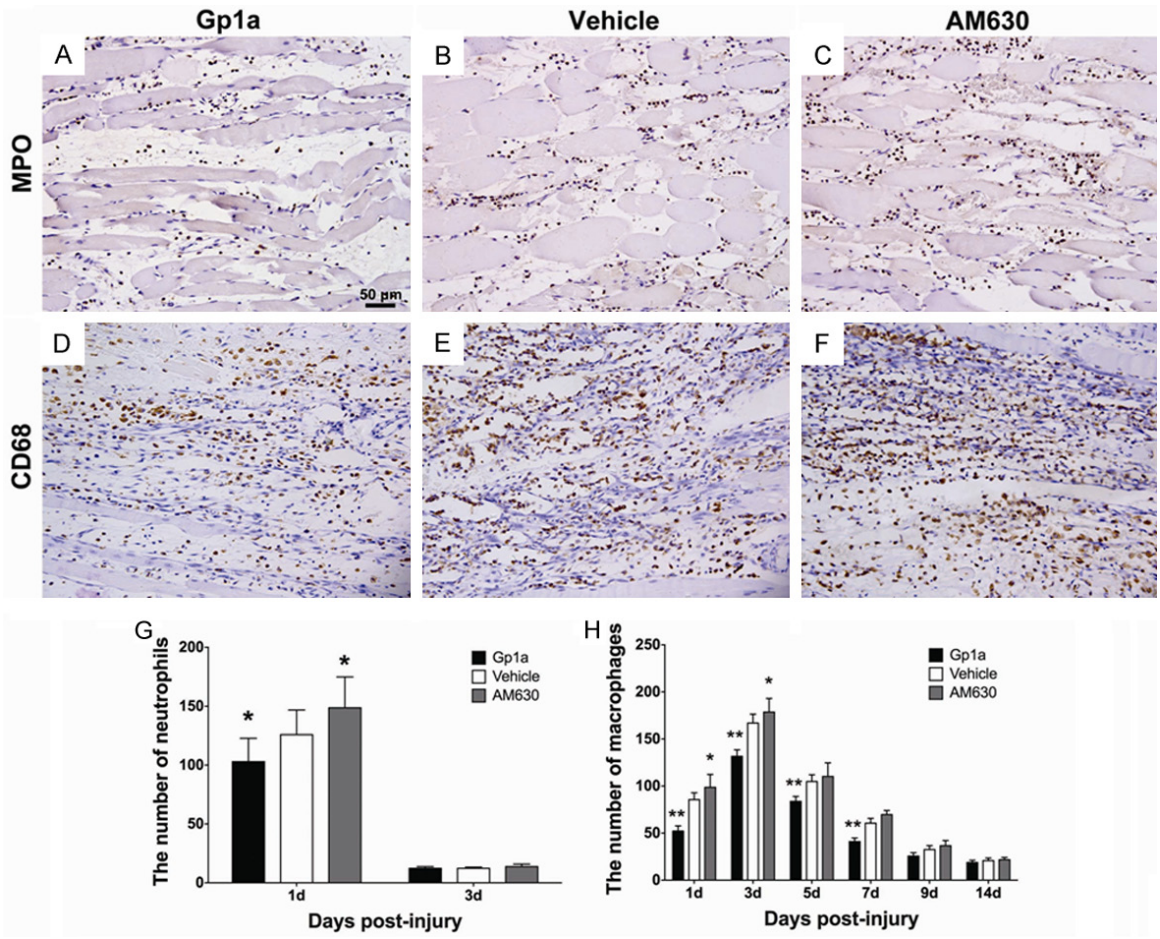

Figure 2. The infiltrated neutrophils and macrophages were identified in the contusion zone by immunohistochemical staining. A-C represent neutrophil infiltration in the Gp1a, Vehicle and AM630 group at 1 day post-injury, respectively. D-F represent macrophage infiltration at 3 days post-injury (original magnification, ×200). The number of neutrophils and macrophages are shown in G and H (under the 400-fold magnification). Data are presented as mean ± SD. **P* < 0.05, ***P* < 0.01 (Gp1a or AM630 vs. Vehicle).

expression at 3, 5 and 7 days post-injury (*P* < 0.01; **Figure 4C**).

Effects of CB2R on fibrosis

Masson's trichrome staining was used to observe and compare the formation of fibrous tissue after injury in the different groups. The results were comparable with those observed after H&E staining. At 9 and 14 days post-injury, the Gp1a-treated group exhibited better recovery and contained less fibrous tissue than the Vehicle-treated groups (*P* < 0.05; **Figure 5A**, **5B**, **5G**). In sharp contrast, muscles from the AM630-treated group contained more fibrous tissue than muscles in the Vehicle-treated group at 9 and 14 days post-injury (*P* < 0.01; **Figure 5B**, **5C**, **5G**).

α-SMA$^+$ cells (myofibroblasts) were observed at 5 days post-injury in all three groups as detected by immunohistochemical staining. The number of myofibroblasts gradually increased with extension of posttraumatic interval. Compared to Vehicle group, myofibroblasts were reduced remarkably in number in the Gp1a group at 7, 9 and 14 days post-injury (*P* < 0.01; **Figure 5D**, **5E**, **5H**), whereas they were significantly increased in the AM630 group at 5 (*P* < 0.05), 7, 9 and 14 days post-injury (*P* < 0.01; **Figure 5E**, **5F**, **5H**).

Quantitative real-time PCR was used to detect and compare the mRNA levels of Collagen I and Collagen III in different groups. Compared to the Vehicle group, a significantly decrease of *Col1a1* level was observed in the Gp1a group at

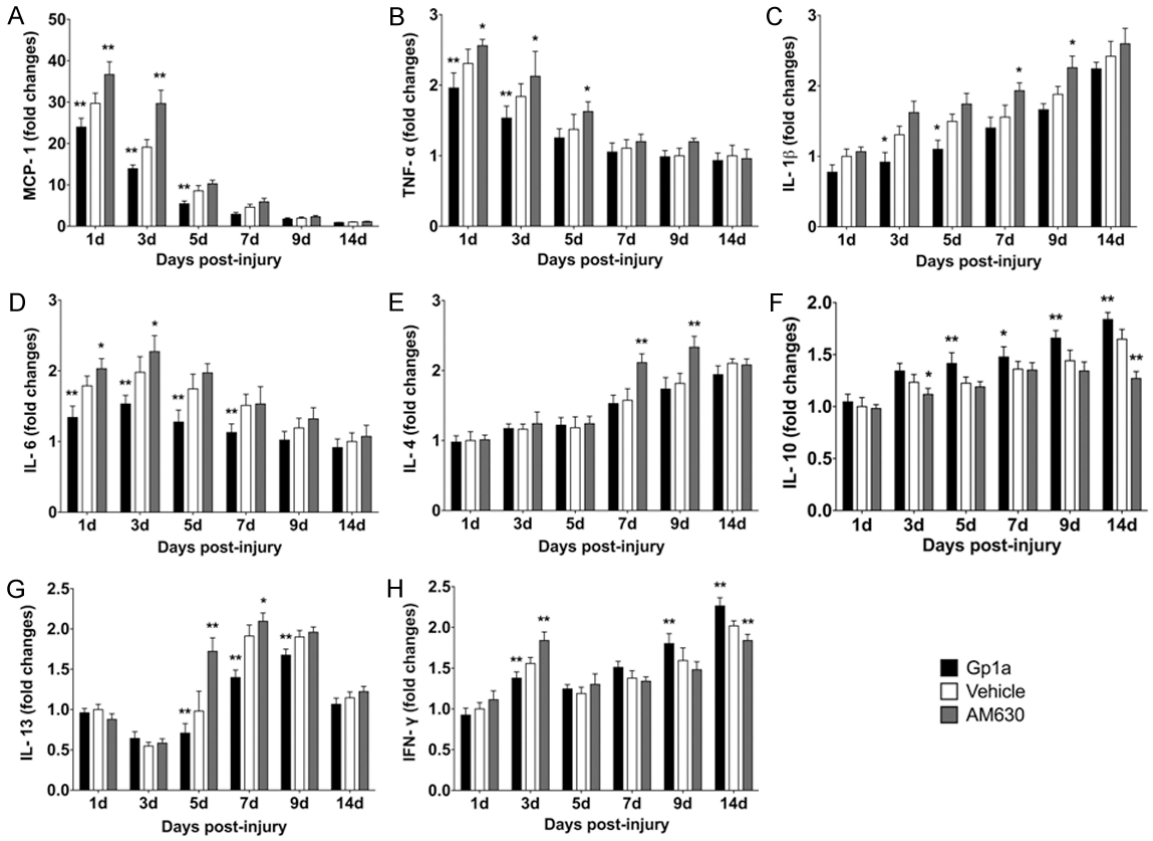

Figure 3. Quantibody Rat Inflammation Array 1 (RayBiotech, Inc, Norcross, GA, USA) was employed to simultaneously determine the expression of MCP-1 (A), TNF-α (B), IL-1β (C), IL-6 (D), IL-4 (E), IL-10 (F), IL-13 (G) and IFN-γ (H). Data are presented as mean ± SD. *$P < 0.05$, **$P < 0.01$ (Gp1a or AM630 vs. Vehicle).

3 and 5 days post-injury ($P < 0.01$; **Figure 6A**), and *Col3a1* level at 3, 5, 7 and 9 days post-injury ($P < 0.01$; **Figure 6B**). Conversely, *Col1a1* and *Col3a1* levels were increased in the AM630 group at 3 and 5 days post-injury ($P < 0.01$; **Figure 6A**), and at 3, 5 and 7 days post-injury ($P < 0.01$; **Figure 6B**), respectively.

Discussion

Skeletal muscle injuries are the most common injuries as caused by strains, contusions, ischemia and neurological dysfunction, all of which present a challenge in primary care and sports medicine [19]. In this study, we used Gp1a and AM630 to evaluate the effects of CB2R on inflammatory process of muscle healing and found that activation of CB2R with Gp1a attenuated both inflammatory response and pro-fibrotic cytokines production during repair of injured skeletal muscles. Conversely, AM630 aggravated inflammatory response and up-regulated the expression of pro-fibrotic cytokines.

When muscles are injured, tissue debris and necrotic cells contribute to the recruitment and activation of inflammatory cells as well as the release of pro-inflammatory cytokines. Inflammation is crucial to the highly orchestrated response to tissue injury. The latest understanding indicates that inflammation persists throughout all wound healing phases, stimulating and coordinating the essential functions of wound repair [20]. As the pro-inflammatory cytokines accumulate, the nearby blood vessel vasodilator are elaborated to increase the cellular traffic in order that neutrophils are drawn by IL-1, TNF-α and other cytokines into the injured area in the early stage of inflammatory response [21, 22]. Following the onset of neutrophil invasion, monocytes begin to invade into the injured area and transform into macrophages by chemokine MCP-1 [23]. Fibroblasts release IFN-γ, which causes monocytes to transform into macrophages [24]. Both neutrophils and macrophages participate in the pro-

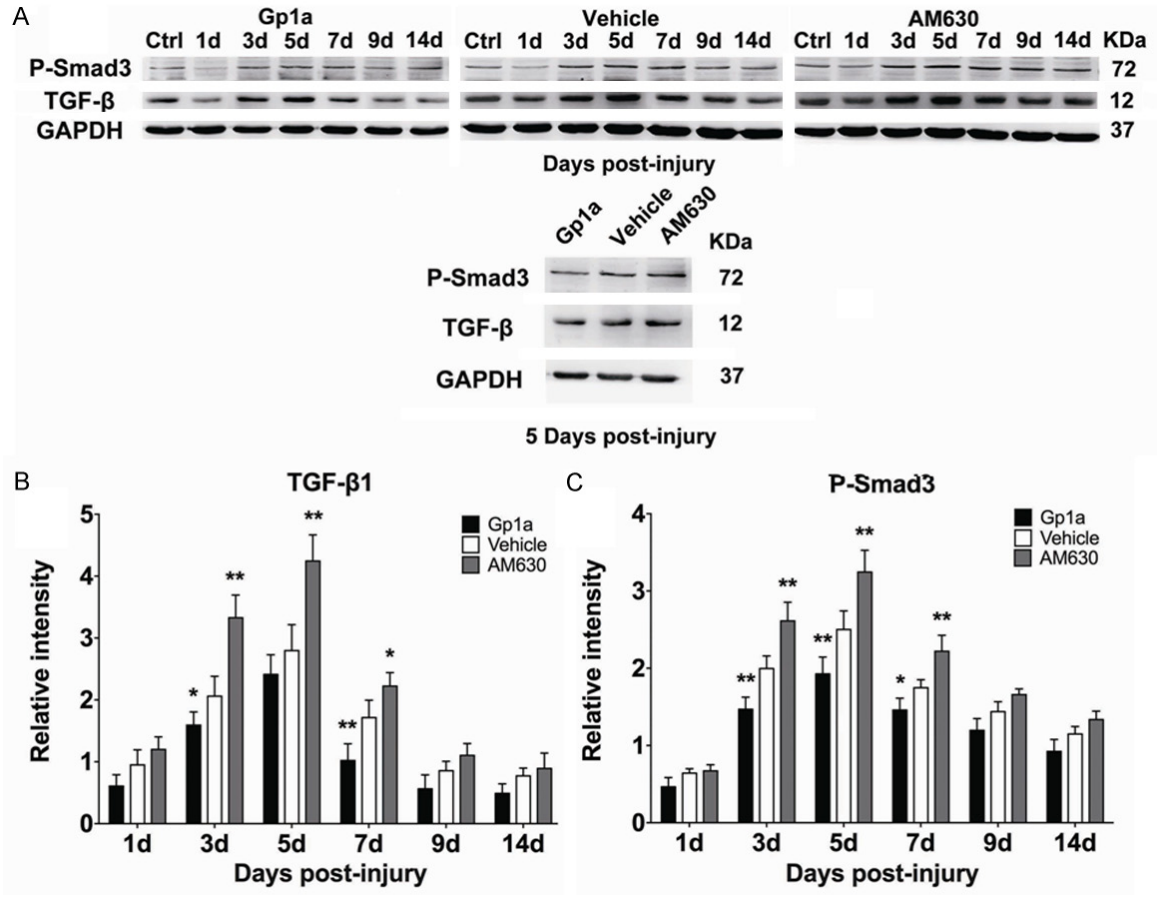

Figure 4. Western blotting was employed to analyze the expression of TGF-β, P-Smad3 and GAPDH. A represents the bands of TGF-β, P-Smad3 and GAPDH in Gp1a, Vehicle and AM630 group, respectively. B and C represent the relative intensities of TGF-β and P-Smad3 to GAPDH. Ctrl were used for normalization. Data are presented as mean ± SD. $*P < 0.05$, $**P < 0.01$ (Gp1a or AM630 vs. Vehicle).

cess of lysing muscle cells, neutrophils may also promote macrophages-mediated cytolysis in a nitric oxide-dependent process in vitro [25]. Besides, TNF-α also plays important roles in activation inflammatory cells which promotes muscle damage and the secretion of the other pro-inflammatory cytokines in injured muscles [26, 27]. MCP-1 is a chemokine that attracts monocytes to the inflammatory site [28] and blockage of MCP-1 leads to a remarkable decrease of macrophage infiltration and TNF-α and IL-6 expression [29, 30]. IL-6 is considered as a cytokine which strongly activates the immune system and enhances inflammatory response [31]. Although inflammatory response process is essential for normal muscle repair, it leads to further damage to uninjured muscles and may be excessive [3]. Excessive and prolonged inflammatory response can delay the regeneration, damage the normal muscle fibers, and even lead to muscle fibrosis, or chronic myoinjury [32].

Since the anti-inflammatory effect of CB2R stimulation has been reported in other inflammation related models, we investigated whether it plays a similar role in our model. MPO and CD68 positive cells were counted for evaluating the neutrophil and macrophage infiltration in the contusion zones. Fewer neutrophils and macrophages appeared in the Gp1a group, but more appeared in the AM630 group. Also, we detected the expression of inflammatory cytokines and found that CB2R stimulation decreased MCP-1, TNF-α, IL-1β, IL-6 and IFN-γ expression in the early stage of inflammation, while CB2R inhibition increased these cytokines expression. The results indicated that CB2R stimulation alleviates inflammatory response by down-regulating the expression of

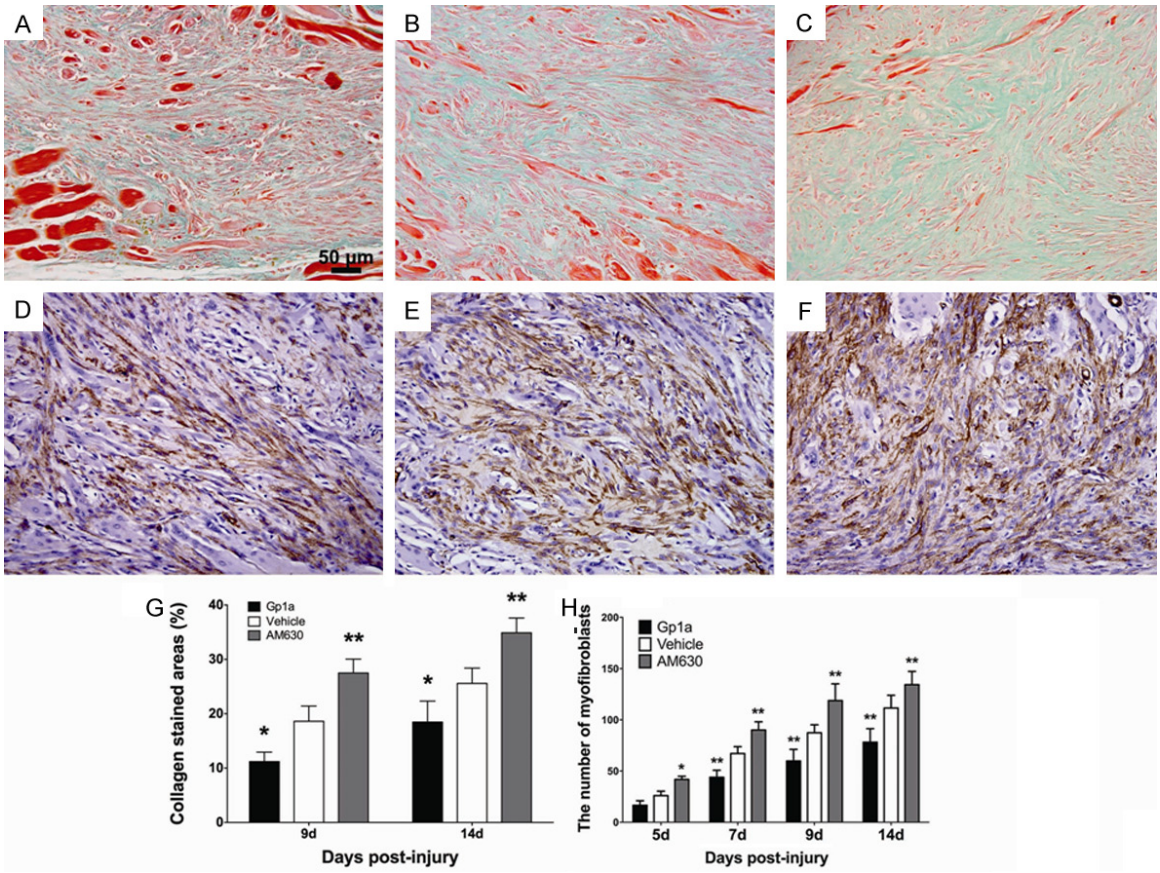

Figure 5. Masson's trichrome staining was applied to observe fibrosis after injury. A-C represent the deposition of collagen in the Gp1a, Vehicle and AM630 group at 14 days post-injury, respectively (original magnification, ×200). The infiltrated myofibroblasts were identified in the contusion zone by immunohistochemical staining. G represents the percentages of fibrosis areas at 9, 14 days post-injury (under the 200-fold magnification). D, E and F represent myofibroblasts infiltration in the Gp1a, Vehicle and AM630 group at 14 day post-injury, respectively (original magnification, ×200). H represents the number of myofibroblasts (under the 400-fold magnification). Data are presented as mean ± SD. $*P < 0.05$, $**P < 0.01$ (Gp1a or AM630 vs. Vehicle).

these mediators and reducing the infiltrated inflammatory cells, while CB2R inhibition aggravates the process.

Fibrosis is an inevitable consequence of wound repair in many organs and tissues. Repair of skeletal muscle injuries is typically an overlapping event between inflammation and tissue repair. Fibrosis is closely related to inflammatory response in wound healing. Macrophages promote fibroblast activation and proliferation by stimulating IL-1β, TGF-β and other cytokines [33]. Meanwhile, fibroblasts summon and stimulate macrophages by producing MCP-1 and other chemokines [34, 35]. In addition, IL-4 and IL-13 are able to activate macrophages, which aggravates inflammation, and they also induce collagen production by fibroblasts [33, 36]. Conversely, IL-10 suppresses immune responses in diverse and independent ways and shut down TGF-β-induced collagen synthesis by fibroblasts [33]. Furthermore, IFN-γ has downregulatory effects on cell proliferation and collagen production in fibroblasts [37]. In this study, we found that CB2R stimulation by Gp1a is able to decrease the expression of pro-fibrotic cytokines MCP-1, IL-1β, IL-4, IL-6, IL-13, and TGF-β with its downstream product P-Smad3, and increasing the expression of anti-fibrotic cytokines IL-10 and IFN-γ. Furthermore, less collagen deposition, myofibroblasts infiltration and *Col1a1/Col3a1* expression were observed in Gp1a-treated group. Converse results were observed in CB2R antagonism group. Therefore, CB2R stimulation might contribute to inhibit the activation and proliferation of fibroblasts by

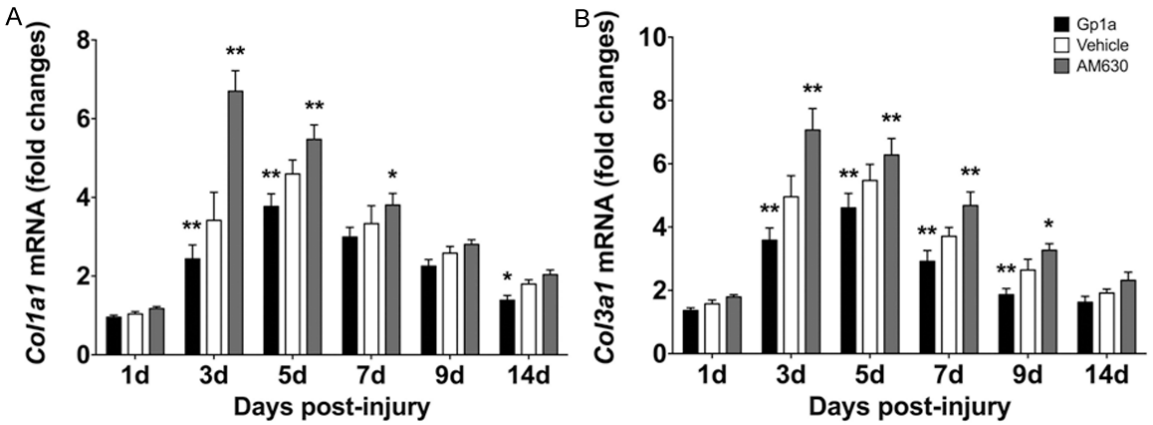

Figure 6. Quantitative real-time PCR was used to analyze the expression of the levels of *Col1a1* and *Col3a1*. A and B represent the dynamic changes of *Col1a1* and *Col3a1*, respectively. Data are presented as mean ± SD. $*P < 0.05$, $**P < 0.01$ (Gp1a or AM630 vs. Vehicle).

regulating the expression of these pro/anti-fibrotic cytokines, which results in reducing the deposition of collagen.

It is noteworthy that intraperitoneal injection of the more potent selective CB2R agonist Gp1a also decreased muscle fibrosis during injured muscles repair, which is consistent with the observation induced by intramuscular injection of JWH-133 in our previous study [9]. The results further demonstrated that CB2R is a potent target to the regulation of fibrogenesis after skeletal muscles injuries.

In summary, our study demonstrates that CB2R is involved in the regulation of inflammatory response in the repair of rat skeletal muscle injuries, and the anti-fibrosis property of CB2R stimulation may be due to the suppression of inflammation and the activation and proliferation of fibroblasts.

Acknowledgements

The study was financially supported in part by grants from research fund for the Doctoral Program funded by Ministry of Education of China (20122104110025) and from projects funded by National Natural Science Foundation of China (81273342) and Shenyang Scientific and Technological Plan (F12-277-1-03).

Disclosure of conflict of interest

None.

Address correspondence to: Dr. Da-Wei Guan, Department of Forensic Pathology, China Medical University School of Forensic Medicine, No. 77, Puhe Road, Shenyang North New Area, Shenyang 110122, Liaoning Province, P. R. China. Tel: +86-24-3193-9433; Fax: +86-24-31939433; E-mail: dwguan@mail.cmu.edu.cn; dwguan@aliyun.com

References

[1] Charge SB and Rudnicki MA. Cellular and molecular regulation of muscle regeneration. Physiol Rev 2004; 84: 209-238.

[2] Prisk V and Huard J. Muscle injuries and repair: the role of prostaglandins and inflammation. Histol Histopathol 2003; 18: 1243-1256.

[3] Paoloni JA, Milne C, Orchard J and Hamilton B. Non-steroidal anti-inflammatory drugs in sports medicine: guidelines for practical but sensible use. Br J Sports Med 2009; 43: 863-865.

[4] Wynn TA. Cellular and molecular mechanisms of fibrosis. J Pathol 2008; 214: 199-210.

[5] Abood ME and Martin BR. Neurobiology of marijuana abuse. Trends Pharmacol Sci 1992; 13: 201-206.

[6] Munoz-Luque J, Ros J, Fernandez-Varo G, Tugues S, Morales-Ruiz M, Alvarez CE, Friedman SL, Arroyo V and Jimenez W. Regression of fibrosis after chronic stimulation of cannabinoid CB2 receptor in cirrhotic rats. J Pharmacol Exp Ther 2008; 324: 475-483.

[7] Galiegue S, Mary S, Marchand J, Dussossoy D, Carriere D, Carayon P, Bouaboula M, Shire D, Le Fur G and Casellas P. Expression of central and peripheral cannabinoid receptors in human immune tissues and leukocyte subpopulations. Eur J Biochem 1995; 232: 54-61.

[8] Yu TS, Cheng ZH, Li LQ, Zhao R, Fan YY, Du Y, Ma WX and Guan DW. The cannabinoid receptor type 2 is time-dependently expressed dur-

ing skeletal muscle wound healing in rats. Int J Legal Med 2010; 124: 397-404.
[9] Yu T, Wang X, Zhao R, Zheng J, Li L, Ma W, Zhang S and Guan D. Beneficial effects of cannabinoid receptor type 2 (CB2R) in injured skeletal muscle post-contusion. Histol Histopathol 2015; [Epub ahead of print]
[10] Gui H, Sun Y, Luo ZM, Su DF, Dai SM and Liu X. Cannabinoid receptor 2 protects against acute experimental sepsis in mice. Mediators Inflamm 2013; 2013: 741303.
[11] Servettaz A, Kavian N, Nicco C, Deveaux V, Chereau C, Wang A, Zimmer A, Lotersztajn S, Weill B and Batteux F. Targeting the cannabinoid pathway limits the development of fibrosis and autoimmunity in a mouse model of systemic sclerosis. Am J Pathol 2010; 177: 187-196.
[12] Mukhopadhyay P, Rajesh M, Pan H, Patel V, Mukhopadhyay B, Batkai S, Gao B, Hasko G and Pacher P. Cannabinoid-2 receptor limits inflammation, oxidative/nitrosative stress, and cell death in nephropathy. Free Radic Biol Med 2010; 48: 457-467.
[13] Akhmetshina A, Dees C, Busch N, Beer J, Sarter K, Zwerina J, Zimmer A, Distler O, Schett G and Distler JH. The cannabinoid receptor CB2 exerts antifibrotic effects in experimental dermal fibrosis. Arthritis Rheum 2009; 60: 1129-1136.
[14] Kisseleva T and Brenner DA. Fibrogenesis of parenchymal organs. Proc Am Thorac Soc 2008; 5: 338-342.
[15] Costola-de-Souza C, Ribeiro A, Ferraz-de-Paula V, Calefi AS, Aloia TP, Gimenes-Junior JA, de Almeida VI, Pinheiro ML and Palermo-Neto J. Monoacylglycerol lipase (MAGL) inhibition attenuates acute lung injury in mice. PLoS One 2013; 8: e77706.
[16] Wang ZY, Wang P and Bjorling DE. Treatment with a cannabinoid receptor 2 agonist decreases severity of established cystitis. J Urol 2014; 191: 1153-1158.
[17] Gamaleddin I, Zvonok A, Makriyannis A, Goldberg SR and Le Foll B. Effects of a selective cannabinoid CB2 agonist and antagonist on intravenous nicotine self administration and reinstatement of nicotine seeking. PLoS One 2012; 7: e29900.
[18] Schmittgen TD, Zakrajsek BA, Mills AG, Gorn V, Singer MJ and Reed MW. Quantitative reverse transcription-polymerase chain reaction to study mRNA decay: comparison of endpoint and real-time methods. Anal Biochem 2000; 285: 194-204.
[19] Baoge L, Van Den Steen E, Rimbaut S, Philips N, Witvrouw E, Almqvist KF, Vanderstraeten G and Vanden Bossche LC. Treatment of skeletal muscle injury: a review. ISRN Orthop 2012; 2012: 689012.
[20] Henry G and Garner WL. Inflammatory mediators in wound healing. Surg Clin North Am 2003; 83: 483-507.
[21] Pohlman TH, Stanness KA, Beatty PG, Ochs HD and Harlan JM. An endothelial cell surface factor(s) induced in vitro by lipopolysaccharide, interleukin 1, and tumor necrosis factor-alpha increases neutrophil adherence by a CDw18-dependent mechanism. J Immunol 1986; 136: 4548-4553.
[22] Bevilacqua MP, Pober JS, Wheeler ME, Cotran RS and Gimbrone MA Jr. Interleukin 1 acts on cultured human vascular endothelium to increase the adhesion of polymorphonuclear leukocytes, monocytes, and related leukocyte cell lines. J Clin Invest 1985; 76: 2003-2011.
[23] Gu L, Tseng SC and Rollins BJ. Monocyte chemoattractant protein-1. Chem Immunol 1999; 72: 7-29.
[24] Broughton G 2nd, Janis JE and Attinger CE. The basic science of wound healing. Plast Reconstr Surg 2006; 117: 12S-34S.
[25] Nguyen HX and Tidball JG. Interactions between neutrophils and macrophages promote macrophage killing of rat muscle cells in vitro. J Physiol 2003; 547: 125-132.
[26] Karalaki M, Fili S, Philippou A and Koutsilieris M. Muscle regeneration: cellular and molecular events. In Vivo 2009; 23: 779-796.
[27] Tidball JG and Villalta SA. Regulatory interactions between muscle and the immune system during muscle regeneration. Am J Physiol Regul Integr Comp Physiol 2010; 298: R1173-1187.
[28] Luster AD. Chemokines--chemotactic cytokines that mediate inflammation. N Engl J Med 1998; 338: 436-445.
[29] Baeck C, Wehr A, Karlmark KR, Heymann F, Vucur M, Gassler N, Huss S, Klussmann S, Eulberg D, Luedde T, Trautwein C and Tacke F. Pharmacological inhibition of the chemokine CCL2 (MCP-1) diminishes liver macrophage infiltration and steatohepatitis in chronic hepatic injury. Gut 2012; 61: 416-426.
[30] Lloyd CM, Minto AW, Dorf ME, Proudfoot A, Wells TN, Salant DJ and Gutierrez-Ramos JC. RANTES and monocyte chemoattractant protein-1 (MCP-1) play an important role in the inflammatory phase of crescentic nephritis, but only MCP-1 is involved in crescent formation and interstitial fibrosis. J Exp Med 1997; 185: 1371-1380.
[31] Wojdasiewicz P, Poniatowski LA and Szukiewicz D. The role of inflammatory and anti-inflammatory cytokines in the pathogenesis of osteoarthritis. Mediators Inflamm 2014; 2014: 561459.
[32] Porter JD, Khanna S, Kaminski HJ, Rao JS, Merriam AP, Richmonds CR, Leahy P, Li J, Guo W and Andrade FH. A chronic inflammatory re-

sponse dominates the skeletal muscle molecular signature in dystrophin-deficient mdx mice. Hum Mol Genet 2002; 11: 263-272.
[33] Barron L and Wynn TA. Fibrosis is regulated by Th2 and Th17 responses and by dynamic interactions between fibroblasts and macrophages. Am J Physiol Gastrointest Liver Physiol 2011; 300: G723-728.
[34] Friedman SL. Hepatic stellate cells: protean, multifunctional, and enigmatic cells of the liver. Physiol Rev 2008; 88: 125-172.
[35] Seki E, De Minicis S, Osterreicher CH, Kluwe J, Osawa Y, Brenner DA and Schwabe RF. TLR4 enhances TGF-beta signaling and hepatic fibrosis. Nat Med 2007; 13: 1324-1332.
[36] Hasegawa M, Fujimoto M, Takehara K and Sato S. Pathogenesis of systemic sclerosis: altered B cell function is the key linking systemic autoimmunity and tissue fibrosis. J Dermatol Sci 2005; 39: 1-7.
[37] Haque MF, Meghji S, Nazir R and Harris M. Interferon gamma (IFN-gamma) may reverse oral submucous fibrosis. J Oral Pathol Med 2001; 30: 12-21.

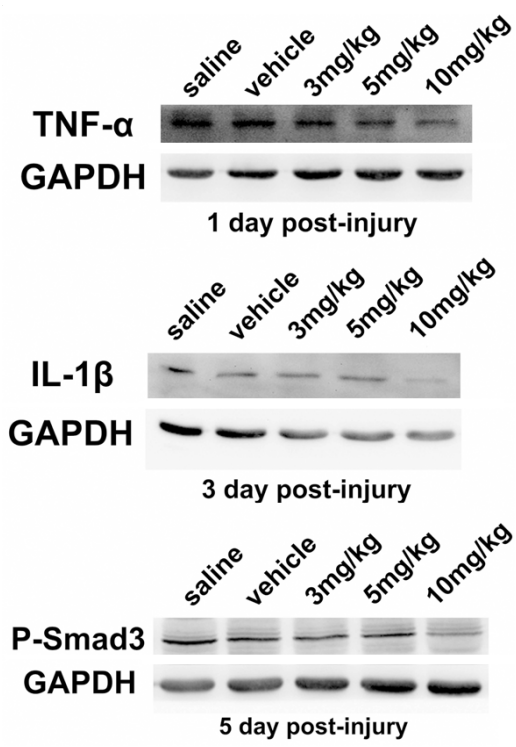

Figure S1. Western-blotting was employed to compare the expressions of TNF-α (dilution 1:500; ab9755, Abcam, Cambridge, UK), IL-1β (dilution 1:500; PAB16928, Abnova, Taipei, Taiwan), P-Smad3 and GAPDH between saline and Vehicle group, and the effects of Gp1a at 3, 5, 10 mg/kg. No significant differences were observed in the expression of TNF-α, IL-1β or P-Smad3 between saline and Vehicle group. Treatment with Gp1a at 10 mg/kg significantly decreased these cytokines production.